TAK1-mediated phosphorylation of PLCE1 represses PIP2 hydrolysis to impede esophageal squamous cancer metastasis

Qianqian Ju[1], Wenjing Sheng[1], Meichen Zhang[1], Jing Chen[1], Liucheng Wu[2], Xiaoyu Liu[1], Wentao Fang[3,*], Hui Shi[3,*], Cheng Sun[1,*]

[1]Key Laboratory of Neuroregeneration of Jiangsu and Ministry of Education; NMPA Key Laboratory for Research and Evaluation of Tissue Engineering Technology Products; School of Medicine, Nantong University, Nantong, 226001, China.

[2]Laboratory Animal Center, Nantong University, Nantong, 226001, China.

[3]Department of Thoracic Surgery, Shanghai Chest Hospital, Shanghai Jiao Tong University School of Medicine, Shanghai, 200030, China.

* Correspondence:

Cheng Sun, Key Laboratory of Neuroregeneration of Jiangsu and Ministry of Education; NMPA Key Laboratory for Research and Evaluation of Tissue Engineering Technology Products; School of Medicine, Nantong University, China. E-mail: suncheng1975@ntu.edu.cn.

Wentao Fang, Department of Thoracic Surgery, Shanghai Chest Hospital, Shanghai Jiao Tong University School of Medicine, Shanghai, China. E-mail: vwtfang@hotmail.com.

Hui Shi, Department of Thoracic Surgery, Shanghai Chest Hospital, Shanghai Jiao Tong University School of Medicine, Shanghai, China. E-mail: shihui1@shchest.org.

Abstract

TAK1, a serine/threonine protein kinase, has been identified as a key regulator in a wide variety of cellular processes. However, its function and involved mechanism in cancer metastasis are still not well understood. Here, we found that knockdown of TAK1 promoted esophageal squamous cancer cell (ESCC) migration and invasion, whereas overexpression of TAK1 resulted in an opposite outcome. Moreover, these *in vitro* findings could be recapitulated *in vivo* in a xenograft metastasis mouse model. Mechanistically, co-immunoprecipitation combined with mass spectrometry demonstrated that TAK1 interacted with phospholipase C epsilon 1 (PLCE1), and phosphorylated PLCE1 at serine 1060 (S1060). Functional studies revealed that phosphorylation at S1060 in PLCE1 resulted in decreased enzyme activity, leading to a repression on PIP2 hydrolysis. As a result, the degradation products of PIP2 including DAG and inositol IP3 were reduced, which thereby suppressed signal transduction in the axis of PKC/GSK-3β/β-Catenin. Consequently, cancer metastasis related genes were impeded by TAK1. Overall, our data indicate that TAK1 plays a negative role in ESCC metastasis, which depends on TAK1 induced phosphorylation of PLCE1 at S1060.

Introduction

Esophageal cancer (EC) is the seventh most common malignancy worldwide with more than 600,000 new cases diagnosed annually (Sung, Ferlay et al., 2021). Clinical survey indicate that EC causes more than 500,000 deaths in 2020 globally (Sung et al., 2021), which is mainly due to its high aggressiveness and poor survival rate. The primary histological subtypes of EC include esophageal squamous cell carcinoma and esophageal adenocarcinoma (He, Xu et al., 2021, Lagergren, Smyth et al., 2017). Esophageal squamous cell carcinoma is a major subtype in China that account for more than 90% of EC (He et al., 2021). Due to the lack of specific biomarkers, the early diagnosis rate of ESCC is very low. Currently, esophageal squamous cell carcinoma diagnosis mainly relies on gastroscopy. By this way, most patients are found to be in locally advanced or metastatic stages when been diagnosed. The 5-year survival rate is approximately 15-25% (Pennathur, Gibson et al., 2013). Surgery has been increasingly used to treat esophageal squamous cell carcinoma at early stages. Neoadjuvant chemotherapy or chemoradiotherapy has become the standard treatment for locally advanced esophageal squamous cell carcinoma (He et al., 2021, Lagergren et al., 2017). In recent decades, therapeutic strategies have made great progress towards esophageal squamous cell carcinoma, and yet recurrence and metastasis are still significant challenges (Mao, Zeng et al., 2021). Therefore, it is urgent to deeply understand the mechanisms involved in cell metastasis, and thus try to explore new druggable targets for treating esophageal squamous cell carcinoma.

Transforming growth factor β-activated kinase 1 (TAK1), a member of the mitogen-activated protein kinase (MAPK) kinase kinase (MAP3K) family, is encoded by the gene *Map3k7*. As a serine/threonine protein kinase, TAK1 has been shown to play an integral role in inflammatory signal transduction across multiple pathways (Sakurai, 2012). By this mean, TAK1 was found to be involved in a wide variety of cellular processes including cell survival, cell migratory and invasive capacity, inflammation, immunity regulation, and tumorigenesis (Cho, Shim et al., 2021, Mukhopadhyay & Lee, 2020). Although TAK1 has been widely studied in cancer progression, its precise role remains controversial. For example, by acting as a tumor suppressor, TAK1 has been shown to negatively associated with tumor progression in several

human cancers including prostate cancer (Huang, Tang et al., 2021), hepatocellular carcinoma (HCC) (Tan, Zhao et al., 2020, Wang, Zhang et al., 2021), cervical cancer (Guan, Lu et al., 2017) and certain blood cancers (Guo, Zhang et al., 2019). On the contrary, TAK1 has been shown to promote tumor progression across a range of human cancers, including colon cancer, ovarian, lung cancer and breast cancer (Augeri, Langenfeld et al., 2016, Cai, Shi et al., 2014, Xu, Niu et al., 2022). The above findings indicate that TAK1 may play a dual role in tumor initiation, progression, and metastasis. In our previous study, TAK1 has been shown to phosphorylate RASSF9 at serine 284 to inhibit cell proliferation by targeting the RAS/MEK/ERK axis in ESCC (Shi, Ju et al., 2021). Up to date, there is no report regarding the precise role of TAK1 on ESCC metastasis.

Phospholipase C epsilon 1 (PLCE1) is encoded by the *Plce1* gene on chromosome 10q23 in human, and belongs to the phospholipase C (PLC) family (Fukami, Inanobe et al., 2010, Kadamur & Ross, 2013). Like other PLC family members, PLCE1 is composed of the PLC catalytic domain, PH domain, EF domain and C2 domain. In addition, PLCE1 also has unique regions, two C-terminal Ras association (RA) domains and a N-terminal CDC25-homology domain (Kadamur & Ross, 2013). Once activated, PLCE1 is essential for intracellular signaling by catalyzing the hydrolysis of membrane phospholipids such as phosphatidylinositol 4,5-bisphosphate (PIP2), to produce two important secondary messengers, inositol 1,4,5-trisphosphate (IP3) and diacylglycerol (DAG), which further trigger IP3-dependent calcium ions (Ca^{2+}) release from the endoplasmic reticulum and PKC activation (Fukami et al., 2010, Kadamur & Ross, 2013). Accumulated evidence has shown that PLCE1 promotes cancer cell growth, migration, and metastasis in multiple human cancers, such as hepatocellular carcinoma, non-small cell lung cancer, head and neck cancer, bladder cancer, gastric cancer, and prostate cancer (Abnet, Freedman et al., 2010, Fan, Fan et al., 2019, Liao, Han et al., 2017, Ma, Wang et al., 2011, Ou, Guo et al., 2010, Wang, Liao et al., 2020, Yue, Zhao et al., 2019). Till now, however, whether and how PLCE1 affects cancer metastasis in ESCC are largely unknown.

In this study, we examined the potential role of TAK1 in cell metastasis in ESCC. We found

that TAK1 negatively regulates cell migration and invasion in ESCC, in which PLCE1 is a downstream target of TAK1. In detail, TAK1 phosphorylates PLCE1 at serine 1060 (S1060) to inhibit its enzyme activity, leading to decreased IP3 and DAG, both are the products of PLCE1 catalyzed reactions. As a result, IP3/DAG triggered signal transduction in the axis of PKC/GSK-3β/β-Catenin was blunted. All these outcomes induced by TAK1 caused a repression on cell migration and invasion in ESCC.

Results

TAK1 negatively regulates ESCC migration and invasion

In our previous study, it has been shown that TAK1 expression was reduced in esophageal squamous tumor tissues, and TAK1 inhibits ESCC proliferation (Shi et al., 2021). To examine whether TAK1 affects the epithelial-mesenchymal transition (EMT) process in ESCC, we increased TAK1 expression in ECA-109 cells by transfecting a plasmid expressing *Map3k7* (TAK1 gene name) and confirmed the overexpression of TAK1 (**Fig. 1A**). Due to the promising roles of epidermal growth factor (EGF) on the EMT (Lu, Ghosh et al., 2003), it was used to trigger the EMT in ESCC. As shown in **Fig. 1B**, EGF treatment induced spindle-shaped cell morphology in ECA-109 cells, which was markedly prevented by TAK1. These data imply that TAK1 is a negative regulator of the EMT in ESCC. To address this prediction, we performed transwell assay and found that TAK1 repressed cell migration and invasion in ECA-109 cells (**Fig. 1C;** *SI Appendix,* Fig. S1A). In addition, wound healing assay further confirmed the negative impact of TAK1 on cancer cell migration (**Fig. 1D;** *SI Appendix,* Fig. S1B). Next, we examined whether TAK1 affects the EMT related gene expression. Our data showed that TAK1 increased E-cadherin and ZO-1, two epithelial molecules, while mesenchymal molecules such as N-cadherin, Vimentin, and ZEB1 were reduced by TAK1 (**Fig. 1E;** *SI Appendix,* Fig. S1C). The qRT-PCR data further confirmed these changes (*SI Appendix,* Fig. S1D).

Next, we performed loss-of-function studies to examine the effects of TAK1 on cell migration and invasion in ESCC. The knockdown efficiency of *Map3k7* siRNA on TAK1 expression was reported previously (Shi et al., 2021). Since the EMT process involves dynamic and spatial

regulation of the cytoskeleton (Fife, McCarroll et al., 2014, Li & Wang, 2020), we therefore analyzed the expression of F-Actin by immunofluorescence. As shown in **Fig. 1F**, TAK1 knockdown induced F-Actin expression. Meanwhile, TAK1 knockdown promoted spindle-shaped mesenchymal morphology in ECA-109 cells (**Fig. 1G**). In accordance to these changes, the cell invasion and migration were stimulated as evidenced by the data from wound healing and transwell assays (**Fig. 1H;** *SI Appendix,* Fig. S2A-B). The epithelial markers including E-cadherin and Claudin-1 were decreased by TAK1 knockdown; while the mesenchymal markers such as N-cadherin, Vimentin, Snail, and Slug were increased (**Fig. 1I**; *SI Appendix,* Fig. S2C). At mRNA level, *Cdh1* and *Cldn1* were inhibited by TAK1 knockdown, while *Cdh2* and *Snail1* were promoted (*SI Appendix,* Fig. S2D). To verify TAK1 knockdown on cell migration and invasion, we also downregulated TAK1 expression by using lentivirus carrying *Map3k7* shRNA (LV-*Map3k7* shRNA) (*SI Appendix,* Fig. S3A, B). In LV-*Map3k7* shRNA transduced cells, cell migration and invasion were obviously increased (*SI Appendix,* Fig. S3C-E). The epithelial markers including E-cadherin, ZO-1, and Claudin-1 were repressed by TAK1 knockdown; while the mesenchymal markers such as N-cadherin, Slug, and ZEB-1 were activated (*SI Appendix,* Fig. S3F, G). The qRT-PCR data showed similar changes in these EMT genes (*SI Appendix,* Fig. S3H). Additionally, TAK1 knockdown was accomplished by CRISPR-Cas9 using *Map3k7* guide RNA (gRNA) (*SI Appendix,* Fig. S4A). Again, we observed cell migration and invasion were enhanced by *Map3k7* gRNA (*SI Appendix,* Fig. S4B-D). The expressions in E-cadherin, ZO-1, and Claudin-1 were inhibited by *Map3k7* gRNA, while the expressions in N-cadherin, Vimentin, Snail, and Slug were activated (*SI Appendix,* Fig. S4E, F). Similar changes in these EMT related gene expression were also observed in qRT-PCR analysis (*SI Appendix,* Fig. S4G). Furthermore, we inhibited TAK1 activity by Oxo, NG25, or Takinib and observed that all these treatments induced morphological changes in ECA-109 cells from round shape to spindle-like shape (*SI Appendix,* Fig. S5A). Cell migration and invasion were also stimulated by TAK1 inhibition (*SI Appendix,* Fig. S5B-E). Taken together, these findings indicate that TAK1 is a negative regulator of cell migration and invasion in ESCC.

TAK1 phosphorylates PLCE1 at serine 1060

The above data clearly showed that TAK1 negatively regulates cell migration and invasion in ESCC. To reveal the involved mechanism, we performed co-immunoprecipitation combined with mass spectrometry to identify the potential downstream target of TAK1. As previously reported, 24 proteins were found to be phosphorylated in the immunocomplex (Shi et al., 2021). Of them, phospholipase C epsilon 1 (PLCE1) caused our attention due to its essential roles in cell growth, migration, and metastasis in various human cancers (Abnet et al., 2010, Chen, Wang et al., 2019, Chen, Xin et al., 2020, Gu, Zheng et al., 2018, Kadamur & Ross, 2013, WangZhou et al., 2010). According to the mass spectrometry data, the serine residue at 1060 (S1060) in PLCE1 was phosphorylated (**Fig. 2A**). Currently, there is no antibody against phosphorylated PLCE1 at S1060 (p-PLCE1 S1060), we therefore generated an antibody for detecting p-PLCE1 S1060. To verify the antibody specificity, S1060 in PLCE1 was mutated into alanine (S1060A). As shown in **Fig. 2B**, wild type (WT) PLCE1 could be phosphorylated by TAK1 at S1060, while PCLE1 S1060A was resistant to TAK1 induced phosphorylation at S1060. Moreover, p-PLCE1 S1060 induced by TAK1 could be weakened by (5Z)-7-Oxozeaenol (Oxo), a potent inhibitor of TAK1 (**Fig. 2C**). Of note, phosphorylated TAK1 (p-TAK1) was markedly decreased in the presence of Oxo, indicating TAK1 was inhibited (**Fig. 2C**). To further confirm these findings, other TAK1 inhibitors such as Takinib and NG25 were employed, and similar changes in p-PLCE1 and p-TAK1 were observed (**Fig. 2D, E**). Collectively, these results indicate that PLCE1 is a downstream target of TAK1, and PLCE1 S1060 was phosphorylated by TAK1. To further confirm this notion, we analyzed TAK1 and p-PCLE1 expression in clinical samples. As shown **Fig. 2F**, TAK1 expression was reduced in tumor tissues as compared to their respective adjacent normal tissues. In accordance to these changes in TAK1, p-PLCE1 was also decreased in tumor tissues (**Fig. 2G**). The Pearson correlation tests showing TAK1 expression was positively correlated with p-PLCE1 (**Fig. 2H**). These changes in TAK1 and p-PLCE1 were recapitulated by western blot data (**Fig. 2I**).

TAK1 phosphorylates PLCE1 to inhibit cell migration and invasion in ESCC

It has been well documented that PLCE1 plays a key role in cancer progression (Abnet et al., 2010, Chen et al., 2019, Chen et al., 2020, Gu et al., 2018, Wang et al., 2010). Therefore, we

predicted that the negative impact of TAK1 on cell migration and invasion in ESCC may rely on PLCE1. To verify this prediction, we first examined whether PLCE1 affects cell migration and invasion. In ECA-109 cells, PLCE1 overexpression significantly increased cell migration and invasion (**Fig. 3A-C**; *SI Appendix*, Fig. S6A, B). In accordance to these changes, the epithelial marker E-cadherin was repressed by PLCE1, while the mesenchymal markers including Vimentin, Snail, Slug, and ZEB-1 were activated (**Fig. 3D**; *SI Appendix,* Fig. S6C). The qRT-PCR data also revealed that *Cdh1* was downregulated by PLCE1, while *Vim*, *Snail1*, and *Snail2* were upregulated (*SI Appendix,* Fig. S6D). To further confirm these findings, we performed PLCE1 knockdown by using siRNA. As shown in **Fig. 3E**, *Plce1* expression was markedly reduced by all three tested siRNAs. Similar changes were also observed in the western blot data (**Fig. 3F**). Of these siRNAs, siRNA-2# exhibited the best knockdown efficiency and it was chosen in the following experiments. On the contrary, as compared to PLCE1 overexpression, PLCE1 knockdown impeded cell migration and invasion (**Fig. 3G, H**; *SI Appendix,* Fig. S7A, B). As for genes in the EMT process, their expressions exhibited contrary patterns with comparison of PLCE1 overexpression (**Fig. 3I**; *SI Appendix,* Fig. S7C, D). Moreover, similar to PLCE1 overexpression, activation of PLCE1 by m-3M3FBS potentiated cell migration and invasion (*SI Appendix,* Fig. S8A-D). Inhibition of PLCE1 by U-73122 recapitulated the phenotypes induced by PLCE1 knockdown (*SI Appendix,* Fig. S9A-D).

Due to PLCE1 is a lipid hydrolase, we next asked whether TAK1-induced phosphorylation in PLCE1 affects its enzyme activity. To this aim, we transfected ECA-109 cells with a plasmid bearing Myc-PLCE1 or TAK1, and PLCE1 was captured by pulldown using anti-Myc beads, which was then subjected to enzyme activity assay. As shown in **Fig. 4A**, the PLCE1 activity was reduced in the presence of TAK1; however, the PLCE1 S1060A activity was not affected (**Fig. 4B**), indicating TAK1 induced phosphorylation at S1060 repressed PLCE1 activity. As a lipid hydrolase, PLCE1 catalyzes PIP2 hydrolysis to produce IP3 and DAG, both are the second messengers in diverse cellular events (Kadamur & Ross, 2013). Therefore, we examined these two products to verify the inhibitory effect of TAK1 on PLCE1. Our data showed that the productions of IP3 and DAG were increased by PLCE1, which could be largely counteracted by TAK1 (**Fig. 4C-E**). As a messenger, IP3 can induce endoplasmic

reticulum to release Ca^{2+} into the cytoplasm (Kadamur & Ross, 2013). Hence, we analyzed the cytoplasmic Ca^{2+} by Fluo-4 AM staining. As expected, the signals for the cytoplasmic Ca^{2+} were obviously increased by PLCE1 in ECA-109 cells, and this trend was weakened by TAK1 (**Fig. 4F, G**). Meanwhile, we also directly detected the cytoplasmic Ca^{2+} with a fluorospectrophotometer and similar changes were observed (**Fig. 4H**). Flow cytometry analysis also evidenced the increase in the cytoplasmic Ca^{2+} induced by PLCE1 was prevented by TAK1 (**Fig. 4I**). All these evidences indicate that TAK1 inhibits PLCE1 activity, which is likely due to TAK1 induced phosphorylation in PLCE1 at S1060. To further verify this notion, a series of functional experiments were performed. For instance, we observed that TAK1 could reverse PLCE1-induced cell migration and invasion; however, TAK1 failed to affect PLCE1 S1060A-induced cell migration and invasion (*SI Appendix,* Fig. S10A-D). Overall, these data clearly indicate that PLCE1 has a positive impact on cell migration and invasion in ESCC. By inducing phosphorylation at S1060, TAK1 inhibits PLCE1 enzyme activity and thereby counteracts PLCE1-induced cell migration and invasion in ESCC. At this regard, PLCE1 is a downstream target of TAK1 for transducing its inhibitory effects on cell migration and invasion in ESCC.

TAK1 inhibits PLCE1-induced signal transduction in the PKC/GSK-3β/β-Catenin axis

PLCE1 hydrolyzes PIP2 to produce two important second messengers DAG and IP3 that trigger Ca^{2+} release from the endoplasmic reticulum to the cytoplasm to activate PKC (Harden, Hicks et al., 2009, Kadamur & Ross, 2013), suggesting PKC activation is responsible for PLCE1-induced cell migration and invasion in ESCC. To address this prediction, we treated cells with 2-APB, an IP3 receptor (IP3R) inhibitor, and found that 2-APB treatment almost completely reversed PLCE1-induced the intracellular Ca^{2+} (*SI Appendix,* Fig. S11A-E). Accordingly, PLCE1-induced cell migration and invasion were also replenished by 2-APB in ECA-109 cells (*SI Appendix,* Fig. S12A-D). The changes in the EMT genes induced by PLCE1 were largely reversed by 2-APB (*SI Appendix,* Fig. S12E). As well as in ECA-109 cells, 2-APB also induced similar phenotypes in KYSE-150 and TE-1 cells (*SI Appendix,* Fig. S13A-E; Fig. S14A-E). Meanwhile, BAPTA-AM, an intracellular Ca^{2+} chelator, was found to be able to dampen PLCE1-induced cell migration and invasion in ECA-109 cells (*SI Appendix,* Fig.

S15A-D). PKC is a promising downstream target of intracellular Ca^{2+} (Kadamur & Ross, 2013). We therefore asked whether PLCE1-induced cell growth behaviors are depended on PKC activation. To this end, Midostaurin was used to inhibit PKC and our data showed that Midostaurin almost completely abolished cell migration and invasion induced by PLCE1 (*SI Appendix,* Fig. S16A-D).

It has been shown that PKC positively regulates the expression and stability of β-Catenin in a GSK-3β-dependent manner (Duong, Yu et al., 2017, Gwak, Cho et al., 2006, Liu, Shi et al., 2018, Ryu & Han, 2015, Tejeda-Munoz, Gonzalez-Aguilar et al., 2015). Of note, β-Catenin is considered as a positive regulator in the EMT process (Valenta, Hausmann et al., 2012). Therefore, we predicted that PLCE1 stimulates cell migration and invasion via the axis of PKC/GSK-3β/β-Catenin. To test this prediction, ECA-109 cells were treated with IP3 receptor (IP3R) inhibitor (2-APB), Ca^{2+} chelator (BAPTA-AM), or PKC inhibitor (Midostaurin), all these treatments successfully inhibited PKC activity as evidenced by reduced phosphorylated PKC (p-PKC) (**Fig. 5A-C**; *SI Appendix,* S17A-C). As a result, phosphorylated GSK-3β (p-GSK3β) was decreased by 2-APB, BAPTA-AM, and Midostaurin (**Fig. 5A-C**; *SI Appendix,* S17A-C), indicating GSK-3β kinase activity was upregulated. Accordingly, phosphorylated β-Catenin (p-β-Catenin) was increased, leading to degradation of β-Catenin (**Fig. 5A-C**; *SI Appendix,* S17A-C). As a downstream target of β-Catenin, MMP2 expression was inhibited by all three tested chemicals (**Fig. 5A-C**; *SI Appendix,* S17A-C). The immunofluorescence data also showed that PLCE1-induced β-Catenin expression could be counteracted by 2-APB, BAPTA-AM, and Midostaurin (**Fig. 5D**). These results clearly indicate that PLCE1-induced cell migration and invasion in ESCC are likely via the axis of PKC/GSK-3β/β-Catenin. Furthermore, we observed that PLCE1-induced signal transduction in the axis of PKC/GSK-3β/β-Catenin could be inhibited by TAK1 (**Fig. 5E**; *SI Appendix,* S17D). The expression of β-Catenin induced by PLCE1 was largely reversed by TAK1 (**Fig. 6F**). However, inactive TAK1 (TAK1 K63W) had no such effects (**Fig. 5G**; *SI Appendix,* S17E). Moreover, TAK1 failed to affect PLCE1 S1060A induced signal cascade in the axis of PKC/GSK-3β/β-Catenin (**Fig. 5H**; *SI Appendix,* S17F). These evidences further indicate that TAK1 phosphorylates PLCE1 at S1060 to inhibit its activity and its downstream signal transduction in the axis of PKC/GSK-3β/β-Catenin.

TAK1 inhibition promotes ESCC metastasis *in vivo*

To examine TAK1-regulated ESCC metastasis *in vivo*, a xenograft model with nude mice was employed. Mice was injected with ECA109 cells via the tail vein, and then mice were daily treated with Takinib (50 mg/kg) or corn oil (Vehicle) for consecutive 15 days. Eight weeks later, mice were sacrificed for analyzing cancer cell metastasis. We found 4 of 6 mice in the Takinib group developed lung metastasis, while only 1 of 6 mice in the Vehicle group had lung metastasis. Moreover, the number of metastatic nodules in lung tissues was higher in Takinib treated mice (**Fig. 6A-C**). In addition, the effects of TAK1 inhibition on the axis of PKC/GSK-3β/β-Catenin was examined. As shown in **Fig. 6D**, TAK1 inhibition by Takinib activated PKC, leading to increased p-GSK-3β. As a result, p-β-Catenin was reduced and MMP2 expression was upregulated (**Fig. 6D, E**). Of note, p-TAK1 was decreased by Takinib, indicating TAK1 activity was successfully inhibited (**Fig. 6D, E**). In accordance to this change, p-PLCE1 was decreased in Takinib-treated mice (**Fig. 6D, E**). Hence, these data indicate that TAK1 represses ESCC metastasis *in vivo*, and this benefit is likely due to TAK1-mediated phosphorylation in PLCE1 at S1060.

PLCE1 facilitates ESCC metastasis *in vivo*

To further verify the function of PLCE1 in ESCC metastasis, we generated a stable cell line with PLCE1 knockdown by using lentivirus bearing PLCE1 shRNA (LV-shPLCE1) (*SI Appendix,* Fig. S18A-B). These cells with low PLCE1 expression were injected into nude mice via the tail vein to produce a mouse xenograft tumor model. Eight weeks later, mice were sacrificed, the nodule number and incidence rate were reduced in mice injected with LV-shPLCE1 cells (**Fig. 7A-C**). In addition, western blot analysis showed that PLCE1 silencing inhibited signal transduction in the PKC/GSK-3β/β-Catenin axis, as evidenced by reduced p-PKC and p-GSK-3β, and increased p-β-Catenin (**Fig. 7D, E**). In accordance to these changes, the expression of MMP2 was decreased (**Fig. 7D, E**). These results further confirmed the notion that PLCE1 plays a key role in cancer cell metastasis in ESCC.

Discussion

TAK1 is a serine/threonine kinase and a major member of the MAPK family (Zhu, Lama et al., 2021). In response to various cytokines, pathogens, lipopolysaccharides, hypoxia, and DNA damage, the E3 ligase TRAF2 or TRAF6 activates TAK1 through Lys63-linked polyubiquitylation, and then TAK1 undergoes auto-phosphorylation at Ser192 and Thr184/187 to achieve full activation (Skaug, Jiang et al., 2009, Sorrentino, Thakur et al., 2008). Consequently, activated TAK1, in turn, phosphorylates downstream substrates to spark the NF-kB and MAPKs (i.e. ERK, p38 MAPK, and JNK) signaling pathways, thereby participates in cellular inflammation, immune response, fibrosis, cell death, and cancer cell invasion and metastasis (Yang, Chen et al., 2022, Zhou, Tao et al., 2021). TAK1 has been shown to decrease in high-grade human prostate cancer; and TAK1 deficiency promotes prostate tumorigenesis by increasing androgen receptor (AR) protein levels and activity or activating p38 MAPK pathway (Huang et al., 2021, Wu, Shi et al., 2012). Similarly, hepatocyte-specific TAK1 ablation drives RIPK1 kinase-dependent inflammation to promote liver fibrosis and hepatocellular carcinoma (Su, Gao et al., 2023, Tan et al., 2020, Xia, Ji et al., 2021). Furthermore, TAK1 represses the transcription of human telomerase; and activate tumor suppressor protein LKB1, all these evidences indicate that TAK1 is a tumor suppressor (Adhikari, Xu et al., 2007, Fujiki, Miura et al., 2007, Xie, Zhang et al., 2006). Consistent with these findings, in our previous study, we found that TAK1 expression was reduced in esophageal squamous tumors compared to adjacent normal tissues, and TAK1 negatively correlates with esophageal squamous tumor patient survival (Shi et al., 2021). In this study, we extended our research on TAK1 and observed that TAK1 inhibits cell migration and invasion in ESCC. In contrast to these findings, TAK1 has been shown to play a positive role in tumor cell proliferation, migration, invasion, colony formation, and metastasis, especially in breast cancer, pancreatic cancer, and non-small cell lung cancer (Kim, Kim et al., 2023, Santoro, Zanotto et al., 2020, Tripathi, Shin et al., 2019). Therefore, TAK1 may play pleiotropic roles in different types of cancer cells.

As a kinase, TAK1 is considered as a central regulator of tumor cell proliferation, migration and invasion and has been demonstrated to play tumor suppression or activation role via the NF-κB and MAPK activation (Mukhopadhyay & Lee, 2020, Wang et al., 2021, Zhang, Cheng et

al., 2023). However, the precise molecular and cellular mechanisms by which TAK1 regulates ESCC metastasis remain unclear. As previously reported, by co-immunoprecipitation coupled with mass spectrometry (MS/MS), we identified RASSF9 as a downstream target of TAK1 for transducing its repression on cell proliferation in ESCC (Shi et al., 2021). By phosphorylating RASSF9 at S284, TAK1 negatively regulates cell proliferation in ESCC (Shi et al., 2021). Meanwhile, we also found that PLCE1 was presented in the immunocomplex, which was phosphorylated at S1060 in the presence of TAK1 in ECA-109 cells. As a member of the human phosphoinositide-specific PLC family, PLCE1 can be activated by a variety of intracellular and extracellular signal molecules including hormones, cytokines, neurotransmitters, growth factors, etc. (Kadamur & Ross, 2013). Numerous studies have shown that PLCE1 plays a key role in cancer development and progression through various pathways (Abnet et al., 2010, Fan et al., 2019, Ghosh, Nataraj et al., 2021, He, Wang et al., 2016, Yue et al., 2019). Moreover, PLCE1 has been characterized as a susceptibility gene in ESCC (Abnet et al., 2010, Wang et al., 2010). All these evidences suggest that PLCE1 is a potential downstream target for transducing the negative impact of TAK1 on cell migration and invasion in ESCC.

Once activated, PLCE1 catalyzes the hydrolysis of PIP2 on the cell membrane to produce two secondary messengers IP3 and DAG; IP3 induces Ca^{2+} release from the ER into the cytoplasm via IP3R; both Ca^{2+} and DAG are potent activators of PKC. By this way, PLCE1 regulates cell growth, proliferation, and differentiation and thereby plays a key role in tumor growth and development (Bunney & Katan, 2010, Kadamur & Ross, 2013, Land & Rubin, 2017, Smrcka, Brown et al., 2012). Consistent with these notions, in this study, we observed that PLCE1-overexpressing cells exhibit higher production of intracellular IP3, DAG, and intracellular Ca^{2+}. As a consequence, we found that PLCE1 overexpression accelerates cell migration and invasion, while PLCE1 knockdown results in an opposite phenotype. Moreover, in the presence of TAK1, PLCE1-induced cell migration and invasion were largely counteracted. By considering TAK1 is a protein kinase, therefore, we proposed that TAK1 phosphorylates PLCE1 at S1060 to inhibit its enzyme activity and thus impedes cell migration and invasion in ESCC. Indeed, PLCE1 activity was blunted in the presence of TAK1, whereas

mutated PLCE1 (PLCE1 S1060A) was not affected. It has been shown that PKC positively regulates the expression and stability of β-Catenin in a GSK-3β-dependent manner (Duong et al., 2017, Gwak et al., 2006, Ryu & Han, 2015). Therefore, we investigated the impact of PLCE1 on the PKC/GSK-3β/β-Catenin axis. As expected, our data revealed that PLCE1 promotes cell migration and invasion in ESCC by activating the PKC/GSK-3β/β-Catenin pathway, results in a series of phosphorylation modification in PKC and GSK-3β. As a result, phosphorylated β-Catenin decreased, leading to higher stability of β-Catenin, which eventually promotes the EMT process by affecting epithelial and mesenchymal gene expression.

In summary, our findings indicate TAK1 is a negative regulator in cell migration and invasion in ESCC. Mechanistically, TAK1 phosphorylates PLCE1 at S1060 to inhibit its phospholipase activity, leading to reductions in IP3 and DAG. Consequently, PKC activity was blunted, which results in decreased phosphorylated GSK-3β and increased phosphorylated β-Catenin. As a consequence, the stability of β-Catenin was decreased and its transcriptional activity was blunted. By this mean, the epithelial marker gene expression was upregulated by TAK1, while the mesenchymal marker gene expression was downregulated. All these outcomes eventually cause a breakdown in cell migration and invasion in ESCC. Hence, our data revealed a new facet of TAK1 in the EMT process in ESCC by inhibiting PLCE1 activity and its downstream signal transduction in the axis of PKC/GSK-3β/β-Catenin. Moreover, TAK1, together with its downstream target PLCE1, are potential druggable targets for developing agents for dealing with ESCC.

Methods

Cell culture

Human ESCC cell lines ECA109, KYSE-150 and TE-1 were purchased from the Shanghai Institute of Biochemistry and Cell Biology (Shanghai, China). HEK-293 cells were purchased from American Type Culture Collection (ATCC, Manassas, VA, USA). All cells were cultured in Dulbecco's modified Eagle's (DMEM) medium (Hyclone, UT, USA) containing 10% fetal bovine serum (FBS, Gibco, Carlsbad, CA), 100 U/ml penicillin and 100 μg/ml streptomycin (Life Technologies, Carlsbad, CA, USA) at 37°C in a humidified atmosphere of 5% CO_2.

Human esophageal squamous tumor specimens

Human esophageal squamous tumor specimens were obtained from the Affiliated Hospital of Nantong University. Human sample collection for research was conducted in accordance with the recognized ethical guideline of Declaration of Helsinki and approved by the Ethics Committee of Affiliated Hospital of Nantong University.

Generation of antibodies against phospho-PLCE1 (S1060)

Rabbit polyclonal antibody that recognizes phospho-PLCE1 (S1060) was raised against c-WSARNPS(p)PGTSAK peptide at Absin (Shanghai, China). Briefly, the phosphorylated polypeptide c-WSARNPS(p)PGTSAK was synthesized as the target peptide. Then two rabbits were immunized with the target peptide antigen. Meanwhile, non-phosphorylated polypeptide c-WSARNPSPGTSAK was synthesized as a control. The rabbits were sacrificed and blood was collected for further purification. The prepared antibody was verified and stored at -20°C until use.

CRISPR-Cas9 mediated TAK1 deletion

Map3k7 was deleted by the method of CRISPR-Cas9 with the procedures describe previously (Shi et al., 2021). Briefly, we designed an integrated vector based on OriP/EBNA1 (epiCRISPR), which bears gRNA, Cas9 and puromycin resistance genes. ECA-109 cells were transfected with the plasmids using Lipofectamine 2000 (Invitrogen) according to the manufacturer's instructions. The cells were cultured in a medium containing 2.5 μg/ml puromycin for 1 week. The surviving stable cells were used for further experiments. The gRNA sequence is listed in Table S1.

Protein extraction and western blot analysis

Western blot assay was performed as previously described (Tan, Krueger et al., 2022). Briefly, Total protein were extracted from cells and tissues using protein lysis buffer supplemented with protease and phosphatase inhibitors (Roche Applied Science, Penzberg, Germany). Protein concentrations were assayed by the Pierce™ BCA Protein Assay Kit (Thermo Scientific,

Waltham, MA, USA). Subsequently, equal amounts of protein were separated with 6% or 10% SDS-PAGE, and then protein were transferred onto 0.45 μm PVDF membranes. After blocked with 5% BSA in TBST for 1 h, the membranes were incubated with primary antibodies at 4°C overnight. Thereafter, the membranes were incubated with HRP-linked secondary antibodies for 1 h at room temperature. Protein signals were visualized using enhanced chemiluminescence (ECL) reagent (Thermo Fisher Scientific, Waltham, MA, USA) and quantitatively analyzed using ImageJ (NIH). Actin were used as a loading control.

Measurement of intracellular-free Ca^{2+}

Cells were transfected with plasmid expressing PLCE1 and/or TAK1 for 6 h and then treated with BAPTA-AM (10 μM), 2-APB (10 μM), or Midostaurin (100 nM) for additional 18 h, respectively. Measurement of intracellular Ca^{2+} in treated cells was performed using a Fluo-4 AM Assay Kit (Beyotime, Jiangsu, China). In detail, cells were washed with PBS, and incubated with 1 μM Fluo-4 AM in PBS at 37°C for 30 min. Cell were then washed with PBS for 3 times and further incubated for 20 min to ensure Fluo-4 AM completely transformed into Fluo-4 in cells. Finally, Fluo-4 fluorescent intensity was detected with a confocal laser scanning fluorescence microscope (Olympus BX51, Tokyo, Japan), fluorescence microplate (BioTek Instruments, Inc.), or flow cytometry (FACSCalibur, BD Bioscience, Franklin Lakes, NJ, USA) at excitation of 488 nm and emission of 520 nm to determine the change of intracellular Ca^{2+} concentration.

PLCE1 pulldown and phospholipase activity assay

Protein pulldown was performed using a previously reported method (Shi et al., 2021). Briefly, HEK293 cells were transfected with a plasmid expressing PLCE1-Myc or TAK1. 24 h post-transfection, cells were harvested for preparing total cell lysates, which was then subjected to protein pulldown assay using the Myc-Tag beads (Sepharose® Bead Conjugate; #55464; CST, Beverley, MA, USA). After 4 h-incubation on a rotator, unbound proteins were removed using the ice-cold wash buffer. Finally, phospholipase activity bound on the beads was detected with a PLC Activity Assay Kit (Jining Shiye, Shanghai, China) with the provided protocol. In rationale, PLC catalyzes the hydrolysis of O-(4-nitrophenyl) choline (NPPC) to

produce p-nitrophenol (PNP), which has an absorption maximum at 405 nm. By detecting the increase rate of PNP at 405 nm, the magnitude of PLC enzyme activity can be calculated.

IP3 and DAG assays

IP3 and DAG levels in cells were assayed by a Human Inositol 1,4,5-triphosphate enzyme-linked Immunosorbent Assay (ELISA) Kit and a Human Diacylglycerol commercial ELISA Kit (Mlbio, Shanghai, China) according to the manufacturer's instructions. The absorbance was measured at 450 nm with a microplate reader.

Co-immunoprecipitation and MS/MS spectrometry

Co-immunoprecipitation and MS/MS assay were performed as previously described (Shi et al., 2021). Briefly, ECA-109 cells were transfected with a plasmid expressing *Map3k7*. 36 h post-transfection, cells were harvested for co-immunoprecipitation by using an antibody against TAK1. The resulting immunocomplex was subjected to LC-MS/MS spectrometry analysis (Shanghai Applied Protein Technology Co., Ltd.). MS/MS spectra were searched using MASCOT engine (Matrix Science, London, UK; version 2.4) against the UniProKB human (161584 total entries, downloaded 20180105).

Mouse xenograft metastasis model

For *in vivo* metastasis assay, 4-week-old male BALB/c nude mice (18-20 g) were purchased from Shanghai Slake Laboratory Animal Co. Ltd. (Shanghai, China) and randomly divided into 2 groups (n = 6 - 10 per group). Mice were housed in air-filtered laminar flow cages (5 mice/cage) with 12 h light cycle and adequate food and water. To examine the role of PLCE1 on metastasis, each mouse was intravenously (i.v.) injected with 1 x 10^6 ECA109 cells diluted in 100 µl PBS, which were transduced with LV-shPLCE1 or negative control virus. Additionally, to examine TAK1 inhibition on metastasis, each mouse was intravenously (i.v.) injected with 1 x 10^6 ECA109 cells. Mice were then intraperitoneally injected with Takinib (50 mg/kg/day) or vehicle (corn oil) for 15 days. Mouse body weight was measured once a week. Eight weeks later, mice were sacrificed, and lungs and livers were collected for further analysis. All animal experiments were carried out in accordance with the institutional ethical guidelines of animal

care, and were approved by the Animal Experimentation Ethics Committee of the Nantong University (Approval ID: SYXK (SU) 2017-0046).

Statistical analysis

Statistical significance of differences between groups were tested by using analysis of variance (ANOVA) or unpaired Student's *t*-test. Data were presented as mean ± SD from at least three independent experiments. All statistical analyses were performed using GraphPad Prism version 8.0 (GraphPad Software, La Jolla, CA, USA). * $p < 0.05$ was accepted as statistical significance.

Data availability

The dataset regarding MS-based protein phosphorylation modifications can be found in Figshare https://doi.org/10.6084/m9.figshare.25271140.

References

Abnet CC, Freedman ND, Hu N, Wang Z, Yu K, Shu XO, Yuan JM, Zheng W, Dawsey SM, Dong LM, Lee MP, Ding T, Qiao YL, Gao YT, Koh WP, Xiang YB, Tang ZZ, Fan JH, Wang C, Wheeler W et al. (2010) A shared susceptibility locus in PLCE1 at 10q23 for gastric adenocarcinoma and esophageal squamous cell carcinoma. *Nat Genet* 42: 764-7

Adhikari A, Xu M, Chen ZJ (2007) Ubiquitin-mediated activation of TAK1 and IKK. *Oncogene* 26: 3214-26

Augeri DJ, Langenfeld E, Castle M, Gilleran JA, Langenfeld J (2016) Inhibition of BMP and of TGFbeta receptors downregulates expression of XIAP and TAK1 leading to lung cancer cell death. *Mol Cancer* 15: 27

Bunney TD, Katan M (2010) Phosphoinositide signalling in cancer: beyond PI3K and PTEN. *Nat Rev Cancer* 10: 342-52

Cai PC, Shi L, Liu VW, Tang HW, Liu IJ, Leung TH, Chan KK, Yam JW, Yao KM, Ngan HY, Chan DW (2014) Elevated TAK1 augments tumor growth and metastatic capacities of ovarian cancer cells through activation of NF-kappaB signaling. *Oncotarget* 5: 7549-62

Chen Y, Wang D, Peng H, Chen X, Han X, Yu J, Wang W, Liang L, Liu Z, Zheng Y, Hu J, Yang L, Li J, Zhou H, Cui X, Li F (2019) Epigenetically upregulated oncoprotein PLCE1 drives esophageal carcinoma angiogenesis and proliferation via activating the PI-PLCepsilon-NF-kappaB signaling pathway and VEGF-C/ Bcl-2 expression. *Mol Cancer* 18: 1

Chen Y, Xin H, Peng H, Shi Q, Li M, Yu J, Tian Y, Han X, Chen X, Zheng Y, Li J, Yang Z, Yang L, Hu J, Huang X, Liu Z, Huang X, Zhou H, Cui X, Li F (2020) Hypomethylation-Linked Activation of PLCE1 Impedes Autophagy and Promotes Tumorigenesis through MDM2-Mediated Ubiquitination and Destabilization of p53. *Cancer Res* 80: 2175-2189

548 Cho SH, Shim HJ, Park MR, Choi JN, Akanda MR, Hwang JE, Bae WK, Lee KH, Sun EG, Chung IJ (2021)
549 Lgals3bp suppresses colon inflammation and tumorigenesis through the downregulation of
550 TAK1-NF-kappaB signaling. *Cell Death Discov* 7: 65
551 Duong M, Yu X, Teng B, Schroder P, Haller H, Eschenburg S, Schiffer M (2017) Protein kinase C ϵ
552 stabilizes beta-catenin and regulates its subcellular localization in podocytes. *J Biol Chem* 292:
553 12100-12110
554 Fan J, Fan Y, Wang X, Niu L, Duan L, Yang J, Li L, Gao Y, Wu X, Luo C (2019) PLCepsilon regulates
555 prostate cancer mitochondrial oxidative metabolism and migration via upregulation of Twist1. *J Exp*
556 *Clin Cancer Res* 38: 337
557 Fife CM, McCarroll JA, Kavallaris M (2014) Movers and shakers: cell cytoskeleton in cancer metastasis.
558 *Br J Pharmacol* 171: 5507-23
559 Fujiki T, Miura T, Maura M, Shiraishi H, Nishimura S, Imada Y, Uehara N, Tashiro K, Shirahata S, Katakura
560 Y (2007) TAK1 represses transcription of the human telomerase reverse transcriptase gene. *Oncogene*
561 26: 5258-66
562 Fukami K, Inanobe S, Kanemaru K, Nakamura Y (2010) Phospholipase C is a key enzyme regulating
563 intracellular calcium and modulating the phosphoinositide balance. *Prog Lipid Res* 49: 429-37
564 Ghosh S, Nataraj NB, Noronha A, Patkar S, Sekar A, Mukherjee S, Winograd-Katz S, Kramarski L, Verma
565 A, Lindzen M, Garcia DD, Green J, Eisenberg G, Gil-Henn H, Basu A, Lender Y, Weiss S, Oren M, Lotem
566 M, Geiger B et al. (2021) PD-L1 recruits phospholipase C and enhances tumorigenicity of lung tumors
567 harboring mutant forms of EGFR. *Cell Rep* 35: 109181
568 Gu D, Zheng R, Xin J, Li S, Chu H, Gong W, Qiang F, Zhang Z, Wang M, Du M, Chen J (2018) Evaluation of
569 GWAS-Identified Genetic Variants for Gastric Cancer Survival. *EBioMedicine* 33: 82-87
570 Guan S, Lu J, Zhao Y, Woodfield SE, Zhang H, Xu X, Yu Y, Zhao J, Bieerkehazhi S, Liang H, Yang J, Zhang F,
571 Sun S (2017) TAK1 inhibitor 5Z-7-oxozeaenol sensitizes cervical cancer to doxorubicin-induced
572 apoptosis. *Oncotarget* 8: 33666-33675
573 Guo D, Zhang A, Huang J, Suo M, Zhong Y, Liang Y (2019) Suppression of HSP70 inhibits the
574 development of acute lymphoblastic leukemia via TAK1/Egr-1. *Biomed Pharmacother* 119: 109399
575 Gwak J, Cho M, Gong SJ, Won J, Kim DE, Kim EY, Lee SS, Kim M, Kim TK, Shin JG, Oh S (2006)
576 Protein-kinase-C-mediated beta-catenin phosphorylation negatively regulates the Wnt/beta-catenin
577 pathway. *J Cell Sci* 119: 4702-9
578 Harden TK, Hicks SN, Sondek J (2009) Phospholipase C isozymes as effectors of Ras superfamily
579 GTPases. *J Lipid Res* 50 Suppl: S243-8
580 He S, Xu J, Liu X, Zhen Y (2021) Advances and challenges in the treatment of esophageal cancer. *Acta*
581 *Pharm Sin B* 11: 3379-3392
582 He Y, Wang C, Wang Z, Zhou Z (2016) Genetic variant PLCE1 rs2274223 and gastric cancer: more to be
583 explored? *Gut* 65: 359-60
584 Huang Z, Tang B, Yang Y, Yang Z, Shi L, Bai Y, Yan B, Karnes RJ, Zhang J, Jimenez R, Wang L, Wei Q, Yang J,
585 Xu W, Jia Z, Huang H (2021) MAP3K7-IKK Inflammatory Signaling Modulates AR Protein Degradation
586 and Prostate Cancer Progression. *Cancer Res* 81: 4471-4484
587 Kadamur G, Ross EM (2013) Mammalian phospholipase C. *Annu Rev Physiol* 75: 127-54
588 Kim MJ, Kim JY, Shin JH, Kang Y, Lee JS, Son J, Jeong SK, Kim D, Kim DH, Chun E, Lee KY (2023) FFAR2
589 antagonizes TLR2- and TLR3-induced lung cancer progression via the inhibition of AMPK-TAK1
590 signaling axis for the activation of NF-kappaB. *Cell Biosci* 13: 102
591 Lagergren J, Smyth E, Cunningham D, Lagergren P (2017) Oesophageal cancer. *Lancet* 390: 2383-2396

592 Land M, Rubin CS (2017) A Calcium- and Diacylglycerol-Stimulated Protein Kinase C (PKC),
593 Caenorhabditis elegans PKC-2, Links Thermal Signals to Learned Behavior by Acting in Sensory
594 Neurons and Intestinal Cells. *Mol Cell Biol* 37
595 Li X, Wang J (2020) Mechanical tumor microenvironment and transduction: cytoskeleton mediates
596 cancer cell invasion and metastasis. *Int J Biol Sci* 16: 2014-2028
597 Liao X, Han C, Qin W, Liu X, Yu L, Zhu G, Yu T, Lu S, Su H, Liu Z, Chen Z, Yang C, Huang K, Liu Z, Liang Y,
598 Huang J, Dong J, Li L, Qin X, Ye X et al. (2017) PLCE1 polymorphisms and expression combined with
599 serum AFP level predicts survival of HBV-related hepatocellular carcinoma patients after hepatectomy.
600 *Oncotarget* 8: 29202-29219
601 Liu T, Shi Y, Chan MTV, Peng G, Zhang Q, Sun X, Zhu Z, Xie Y, Sham KWY, Li J, Liu X, Ho IHT, Gin T, Lu Z,
602 Wu WKK, Cheng CHK (2018) Developmental protein kinase C hyper-activation results in microcephaly
603 and behavioral abnormalities in zebrafish. *Transl Psychiatry* 8: 232
604 Lu Z, Ghosh S, Wang Z, Hunter T (2003) Downregulation of caveolin-1 function by EGF leads to the loss
605 of E-cadherin, increased transcriptional activity of beta-catenin, and enhanced tumor cell invasion.
606 *Cancer Cell* 4: 499-515
607 Ma H, Wang LE, Liu Z, Sturgis EM, Wei Q (2011) Association between novel PLCE1 variants identified in
608 published esophageal cancer genome-wide association studies and risk of squamous cell carcinoma of
609 the head and neck. *BMC Cancer* 11: 258
610 Mao C, Zeng X, Zhang C, Yang Y, Xiao X, Luan S, Zhang Y, Yuan Y (2021) Mechanisms of Pharmaceutical
611 Therapy and Drug Resistance in Esophageal Cancer. *Front Cell Dev Biol* 9: 612451
612 Mukhopadhyay H, Lee NY (2020) Multifaceted roles of TAK1 signaling in cancer. *Oncogene* 39:
613 1402-1413
614 Ou L, Guo Y, Luo C, Wu X, Zhao Y, Cai X (2010) RNA interference suppressing PLCE1 gene expression
615 decreases invasive power of human bladder cancer T24 cell line. *Cancer Genet Cytogenet* 200: 110-9
616 Pennathur A, Gibson MK, Jobe BA, Luketich JD (2013) Oesophageal carcinoma. *Lancet* 381: 400-12
617 Ryu JM, Han HJ (2015) Autotaxin-LPA axis regulates hMSC migration by adherent junction disruption
618 and cytoskeletal rearrangement via LPAR1/3-dependent PKC/GSK3beta/beta-catenin and PKC/Rho
619 GTPase pathways. *Stem Cells* 33: 819-32
620 Sakurai H (2012) Targeting of TAK1 in inflammatory disorders and cancer. *Trends Pharmacol Sci* 33:
621 522-30
622 Santoro R, Zanotto M, Simionato F, Zecchetto C, Merz V, Cavallini C, Piro G, Sabbadini F, Boschi F,
623 Scarpa A, Melisi D (2020) Modulating TAK1 Expression Inhibits YAP and TAZ Oncogenic Functions in
624 Pancreatic Cancer. *Mol Cancer Ther* 19: 247-257
625 Shi H, Ju Q, Mao Y, Wang Y, Ding J, Liu X, Tang X, Sun C (2021) TAK1 Phosphorylates RASSF9 and
626 Inhibits Esophageal Squamous Tumor Cell Proliferation by Targeting the RAS/MEK/ERK Axis. *Adv Sci*
627 *(Weinh)* 8: 2001575
628 Skaug B, Jiang X, Chen ZJ (2009) The role of ubiquitin in NF-kappaB regulatory pathways. *Annu Rev*
629 *Biochem* 78: 769-96
630 Smrcka AV, Brown JH, Holz GG (2012) Role of phospholipase Cepsilon in physiological
631 phosphoinositide signaling networks. *Cell Signal* 24: 1333-43
632 Sorrentino A, Thakur N, Grimsby S, Marcusson A, von Bulow V, Schuster N, Zhang S, Heldin CH,
633 Landstrom M (2008) The type I TGF-beta receptor engages TRAF6 to activate TAK1 in a receptor
634 kinase-independent manner. *Nat Cell Biol* 10: 1199-207
635 Su W, Gao W, Zhang R, Wang Q, Li L, Bu Q, Xu Z, Liu Z, Wang M, Zhu Y, Wu G, Zhou H, Wang X, Lu L

636 (2023) TAK1 deficiency promotes liver injury and tumorigenesis via ferroptosis and macrophage
637 cGAS-STING signalling. *JHEP Rep* 5: 100695
638 Sung H, Ferlay J, Siegel RL, Laversanne M, Soerjomataram I, Jemal A, Bray F (2021) Global Cancer
639 Statistics 2020: GLOBOCAN Estimates of Incidence and Mortality Worldwide for 36 Cancers in 185
640 Countries. *CA Cancer J Clin* 71: 209-249
641 Tan R, Krueger RK, Gramelspacher MJ, Zhou X, Xiao Y, Ke A, Hou Z, Zhang Y (2022) Cas11 enables
642 genome engineering in human cells with compact CRISPR-Cas3 systems. *Mol Cell* 82: 852-867 e5
643 Tan S, Zhao J, Sun Z, Cao S, Niu K, Zhong Y, Wang H, Shi L, Pan H, Hu J, Qian L, Liu N, Yuan J (2020)
644 Hepatocyte-specific TAK1 deficiency drives RIPK1 kinase-dependent inflammation to promote liver
645 fibrosis and hepatocellular carcinoma. *Proc Natl Acad Sci U S A* 117: 14231-14242
646 Tejeda-Munoz N, Gonzalez-Aguilar H, Santoyo-Ramos P, Castaneda-Patlan MC, Robles-Flores M (2015)
647 Glycogen Synthase Kinase 3beta Is Positively Regulated by Protein Kinase Czeta-Mediated
648 Phosphorylation Induced by Wnt Agonists. *Mol Cell Biol* 36: 731-41
649 Tripathi V, Shin JH, Stuelten CH, Zhang YE (2019) TGF-beta-induced alternative splicing of TAK1
650 promotes EMT and drug resistance. *Oncogene* 38: 3185-3200
651 Valenta T, Hausmann G, Basler K (2012) The many faces and functions of beta-catenin. *EMBO J* 31:
652 2714-36
653 Wang L, Zhang X, Lin ZB, Yang PJ, Xu H, Duan JL, Ruan B, Song P, Liu JJ, Yue ZS, Fang ZQ, Hu H, Liu Z,
654 Huang XL, Yang L, Tian S, Tao KS, Han H, Dou KF (2021) Tripartite motif 16 ameliorates nonalcoholic
655 steatohepatitis by promoting the degradation of phospho-TAK1. *Cell Metab* 33: 1372-1388 e7
656 Wang LD, Zhou FY, Li XM, Sun LD, Song X, Jin Y, Li JM, Kong GQ, Qi H, Cui J, Zhang LQ, Yang JZ, Li JL, Li
657 XC, Ren JL, Liu ZC, Gao WJ, Yuan L, Wei W, Zhang YR et al. (2010) Genome-wide association study of
658 esophageal squamous cell carcinoma in Chinese subjects identifies susceptibility loci at PLCE1 and
659 C20orf54. *Nat Genet* 42: 759-63
660 Wang XK, Liao XW, Yang CK, Liu ZQ, Han QF, Zhou X, Zhang LB, Deng T, Gong YZ, Huang JL, Huang R,
661 Han CY, Yu TD, Su H, Ye XP, Peng T, Zhu GZ (2020) Oncogene PLCE1 may be a diagnostic biomarker and
662 prognostic biomarker by influencing cell cycle, proliferation, migration, and invasion ability in
663 hepatocellular carcinoma cell lines. *J Cell Physiol* 235: 7003-7017
664 Wu M, Shi L, Cimic A, Romero L, Sui G, Lees CJ, Cline JM, Seals DF, Sirintrapun JS, McCoy TP, Liu W, Kim
665 JW, Hawkins GA, Peehl DM, Xu J, Cramer SD (2012) Suppression of Tak1 promotes prostate
666 tumorigenesis. *Cancer Res* 72: 2833-43
667 Xia S, Ji L, Tao L, Pan Y, Lin Z, Wan Z, Pan H, Zhao J, Cai L, Xu J, Cai X (2021) TAK1 Is a Novel Target in
668 Hepatocellular Carcinoma and Contributes to Sorafenib Resistance. *Cell Mol Gastroenterol Hepatol* 12:
669 1121-1143
670 Xie M, Zhang D, Dyck JR, Li Y, Zhang H, Morishima M, Mann DL, Taffet GE, Baldini A, Khoury DS,
671 Schneider MD (2006) A pivotal role for endogenous TGF-beta-activated kinase-1 in the
672 LKB1/AMP-activated protein kinase energy-sensor pathway. *Proc Natl Acad Sci U S A* 103: 17378-83
673 Xu G, Niu L, Wang Y, Yang G, Zhu X, Yao Y, Zhao G, Wang S, Li H (2022) HDAC6-dependent deacetylation
674 of TAK1 enhances sIL-6R release to promote macrophage M2 polarization in colon cancer. *Cell Death*
675 *Dis* 13: 888
676 Yang L, Chen H, Hu Q, Liu L, Yuan Y, Zhang C, Tang J, Shen X (2022) Eupalinolide B attenuates
677 lipopolysaccharide-induced acute lung injury through inhibition of NF-kappaB and MAPKs signaling by
678 targeting TAK1 protein. *Int Immunopharmacol* 111: 109148
679 Yue QY, Zhao W, Tan Y, Deng XL, Zhang YH (2019) PLCE1 inhibits apoptosis of non-small cell lung cancer

via promoting PTEN methylation. *Eur Rev Med Pharmacol Sci* 23: 6211-6216

Zhang X, Cheng L, Gao C, Chen J, Liao S, Zheng Y, Xu L, He J, Wang D, Fang Z, Zhang J, Yan M, Luan Y, Chen S, Chen L, Xia X, Deng C, Chen G, Li W, Liu Z et al. (2023) Androgen Signaling Contributes to Sex Differences in Cancer by Inhibiting NF-kappaB Activation in T Cells and Suppressing Antitumor Immunity. *Cancer Res* 83: 906-921

Zhou Y, Tao T, Liu G, Gao X, Gao Y, Zhuang Z, Lu Y, Wang H, Li W, Wu L, Zhang D, Hang C (2021) TRAF3 mediates neuronal apoptosis in early brain injury following subarachnoid hemorrhage via targeting TAK1-dependent MAPKs and NF-kappaB pathways. *Cell Death Dis* 12: 10

Zhu L, Lama S, Tu L, Dusting GJ, Wang JH, Liu GS (2021) TAK1 signaling is a potential therapeutic target for pathological angiogenesis. *Angiogenesis* 24: 453-470

Acknowledgements

We would like to thank Friedhelm Hildebrandt from University of Michigan Drive for providing the plasmid expressing PLCE1. This work was supported by the National Natural Science Foundation of China (No. 32271193); the Natural Science Foundation of Shanghai (No. 21ZR1449800); the Scientific Project from Shanghai Municipal Health Commission (202240015); the Postgraduate Research & Practice Innovation Program of Jiangsu Province (KYCX23_3411); and the Priority Academic Program Development (PAPD) of Jiangsu Higher Education Institutions.

Author contributions

QJ performed all the experiments with assistance from WS, MZ, and JC. XL designed oligonucleotide sequences for qRT-PCR, shRNA, siRNA, and mutated PLCE1. LW provided advice throughout the development of the project. CS, TW, and HS developed the study concept and experiment design, supervised the study, and wrote the manuscript with input from all the authors.

Disclosure and competing interest statement

The authors declare that they have no competing interests.

Figure legends

Figure 1. TAK1 negatively regultes ESCC migration and invasion

(A) Increased expression of TAK1 in ECA-109 cells transfected with a plasmid expressing *Map3k7*.

(B) Increased expression of TAK1 inhibits the morphological changes to form spindle-shaped mesenchymal cells induced by EGF (100 ng/ml) in ECA-109. Scale bar = 100 µm.

(C) Increased expression of TAK1 inhibits cell migration and invasion in ECA-109 cells. Cell migration and invasion were analyzed by transwell assay. Scale bar = 500 µm. n = 4 biologically independent replicates.

(D) Wound healing assay showing cell migration was attenuated by TAK1. n = 5 biologically independent replicates.

(E) TAK1 decreased mesenchymal marker gene expression, while increased the expression of epithelial markers. ECA-109 cells were transfected with the plasmid carrying *Map3k7*. 24 h post-transfection, protein samples were prepared and subjected to western blot. Actin was used as a loading control.

(F) Knockdown of TAK1 increased the expression of F-Actin. ECA-109 cells were transfected with *Map3k7* siRNA. Seventy-two h post-transfection, cells were subjected to immunofluorescence analysis using an anti-F-Actin antibody (red). Hoechst was used to stain the nucleus (blue). Scale bar = 100 µm.

(G) TAK1 knockdown induces spindle-shaped mesenchymal cell morphology in ECA-109 cells. Scale bar = 100 µm.

(H) Reduced expression of TAK1 promotes cell migration and invasion. ECA-109 cells were transfected with *Map3k7* siRNA. 72 h post-transfection, cell migration and invasion were analyzed by transwell assay. n = 5 biologically independent replicates.

(I) Knockdown of TAK1 increases mesenchymal protein marker expression, and decreases epithelial protein marker expression.

Data are presented as mean ± SD. Statistical significance was tested by unpaired Student's *t*-test. $^{*}p < 0.05$, $^{**}p < 0.01$, and $^{***}p < 0.001$.

Figure 2. TAK1 phosphorylates PLCE1 at serine 1060

(A) Tandem mass spectrometry showing serine 1060 (S1060) in PLCE1 was phosphorylated by TAK1. ECA-109 cells were transfected with a plasmid expressing *Map3k7*. Twenty-four h-post transfection, cells were harvested and subjected to co-immunoprecipitation. The resulting immunocomplex was analyzed by liquid chromatography coupled with tandem mass spectrometry (LC-MS/MS).

(B) TAK1 fails to phosphorylate PLCE1^{S1060A}. ECA-109 cells were co-transfected with the plasmids carrying wildtype (WT) *Plce1*, mutated *Plce1* (PLCE1^{S1060A}), or *Map3k7* as indicated. Twenty-four h-post transfection, cells were collected for western blot analysis.

(C-E) Inhibition of TAK1 reduces PLCE1 phosphorylation at S1060. ECA-109 cells were co-transfected with the plasmids expressing *Plce1* or *Map3k7*. 6 h post-transfection, TAK1 inhibitor (5Z)-7-Oxozeaenol (Oxo; 10 μM) (C), or 10 μM Takinib (D), or 10 μM NG25 (E) was added in culture medium, and cells were cultured for additional 18 h. Cells were then subjected to western blot analysis. Actin was used as a loading control.

(F-G) Immunohistochemical analysis of TAK1 (F) and p-PLCE1 (G) expression in normal and esophageal squamous tumor tissues. *n* = 4 biologically independent replicates. Scale bar = 20 μm.

(H) Correlation between p-PLCE1 and TAK1 based on immunohistochemical data as shown in (F-G). 10 views for each sample were randomly chosen for Pearson correlation test.

(I) TAK1 and p-PLCE1 protein levels in clinical samples. Protein levels were analyzed by western blot, and Actin was used as a loading control. *n* = 4 biologically independent replicates. N: normal tissue; T: tumor tissue.

Figure 3. PLCE1 positively regulates ESCC migration and invasion

(A) Increased expression of PLCE1 in ECA-109 cells transfected with a plasmid expressing *Plce1*.

(B-C) Increased expression of PLCE1 enhances cell migration and invasion. ECA-109 cells were transfected with the plasmid carrying *Plce1*. Twenty-four h-post transfection, cells were subjected to transwell (B) or wound healing (C) assay. *n* = 5 biologically independent replicates.

(D) Increased expression of PLCE1 in ECA-109 cells induces mesenchymal protein marker

expression, while reduces epithelial protein marker expression.

(E-F) Knockdown of PLCE1. ECA-109 cells were transfected with siRNAs targeting *Plce1*. Seventy-two h-post transfection, cells were harvested for analyzing PLCE1 expression by qRT-PCR (E) and western blot (F).

(G-H) Reduced expression of PLCE1 inhibits cell migration and invasion. ECA-109 cells were transfected with *Plce1* siRNA-2. Forty-eight h-post transfection, cells were subjected to transwell (G) or wound healing (H) assay. *n* = 3-5 biologically independent replicates.

(I) Knockdown of PLCE1 promotes epithelial protein marker expression, while represses mesenchymal protein marker expression. ECA-109 cells were transfected with *Plce1* siRNA-2. Seventy-two h-post transfection, cells were harvested and subjected to western blot analysis. Protein level was detected by western blot, and Actin was used as a loading control. Gene expression was analyzed by qRT-PCR and *Gapdh* was used as a house-keeping gene. Data are presented as mean ± SD. Statistical significance was tested by unpaired Student's *t*-test. $*p < 0.05$, $**p < 0.01$, and $***p < 0.001$.

Figure 4. TAK1 inhibits PLCE1 enzyme activity

(A-B) Effects of TAK1 on PLCE1 (A) and PLCE1 S1060A (B) enzyme activity. ECA-109 cells were co-transfected with the plasmids expressing *Plce1-Myc* or *Map3k7*. Twenty-four h post-transfection, cells were subjected to pull down assay by using the beads with anti-Myc antibody. PLCE1 enzyme activity was assayed by Phospholipases C (PLC) Activity Assay Kit. *n* = 3 biologically independent replicates.

(C-E) TAK1 abolishes PLCE1-induced IP3 and DAG in ECA-109 (C), KYSE-150 (D), and TE-1 cells (E). Cells were transfected with the plasmids bearing *Plce1* or *Map3k7* as indicated. Twenty-four h post-transfection, cells were harvested for measuring IP3 and DAG. *n* = 3 biologically independent replicates.

(F) TAK1 attenuates PLCE1-induced intracellular Ca^{2+} ($[Ca^{2+}]$). ECA-109 cells were transfected with the plasmids bearing *Plce1* or *Map3k7* as indicated. $[Ca^{2+}]$ was labeled with Fluo-4 AM, which was then detected by a fluorescent microscope. Scale bar = 200 µm.

(G) Quantified fluorescence intensity of $[Ca^{2+}]$ in ECA-109 cells. *n* = 3 biologically independent replicates.

(H) Fluorescence intensity of Fluo-4 in ECA-109, KYSE-150, and TE-1 cells was examined with a fluorospectrophotometer. *n* = 3 biologically independent replicates.

(I) Flow cytometry analysis of [Ca^{2+}]. Cell treatments were described in (F).

Data are presented as mean ± SD. Statistical significance was tested by unpaired Student's *t*-test (A-B) or two-tailed one-way ANOVA test (C-E, G-I). $*p < 0.05$, $**p < 0.01$, and $***p < 0.001$.

Figure 5. TAK1 inhibits PLCE1-induced signal transduction in the axis of PKC/GSK-3β/β-Catenin

(A) IP3R blocking inhibits PLCE1 induced signal transduction in the axis of PKC/GSK-3β/β-Catenin. ECA-109 cells were transfected with the plasmid expressing *Plce1* for 6 h and then treated with 2-APB (10 μM) for additional 18 h.

(B) [Ca^{2+}] blocking represses signal transduction in the axis of PKC/GSK-3β/β-Catenin induced by PLCE1. ECA-109 cells were transfected with the plasmid expressing *Plce1* for 6 h and then treated with BAPTA-AM (10 μM) for additional 18 h.

(C) PKC inhibition blocks PLCE1 stimulated signal transduction in the axis of PKC/GSK-3β/β-Catenin. ECA-109 cells were transfected with the plasmid expressing *Plce1*. 6 h post-transfection, cells were treated with 100 nM of Midostaurin for additional 18 h.

(D) PKC inhibition represses PLCE1-induced nuclear translocation of β-Catenin in ECA-109 cells. Cells were transfected with the plasmid expressing PLCE1. Six h post-transfection, 2-APB (10 μM), BAPTA-AM (10 μM), or Midostaurin (100 nM) was added in culture medium, and cells were cultured for additional 18 h. Scale bar = 100 μm. Immunofluorescence was used to examine subcellular distribution of β-Catenin.

(E) TAK1 counteracts PLCE1-induced signal transduction in the axis of PKC/GSK-3β/β-Catenin. ECA-109 cells were transfected with the plasmids expressing *Plce1* or *Map3k7* as indicated for 24 h.

(F) TAK1 reduces PLCE1-induced nuclear distribution of β-Catenin in ECA-109 cells. Cells were transfected with the plasmids expressing *Plce1* or *Map3k7* as indicated. Scale bar = 100 μm.

(G) Dominant negative TAK1 (K63W) fails to block signal transduction in the axis of PKC/GSK-3β/β-Catenin/MMP2 induced by PLCE1. ECA-109 cells were transfected with the plasmids expressing *Plce1* or mutated *Map3k7* (TAK1 K63W) for 24 h.

(H) TAK1 has no effect on PLCE1 S1060A induced signal transduction in the axis of PKC/GSK-3β/β-Catenin. ECA-109 cells were transfected with the plasmids expressing PLCE1 S1060A or TAK1 for 24 h. Protein levels were analyzed by western blot, and Actin was used as a loading control. Representative blots were shown.

Figure 6. Inhibition of TAK1 by Takinib promotes ESCC metastasis in nude mice

Each mouse was intravenously injected with 1 x 10^6 ECA109 cells diluted in 100 μl PBS. Mice were treated with Takinib at the dosage of 50 mg/kg/day for 15 days, mice in control group were received vehicle (corn oil). Eight weeks later, mice were sacrificed, and the lungs and livers from each group were collected and photographed.

(A) Typical images of specimens.

(B) Hematoxylin and eosin staining of metastatic nodules in lungs.

(C) The number of nodules in lungs.

(D) Takinib treatment induces signal transduction in the axis of PKC/GSK-3β/β-Catenin. Protein levels were analyzed by western blot, and Actin was used as a loading control. $n = 3$ biologically independent replicates.

(E) Quantitative analysis of the western blot data shown in (D).

Data are presented as mean ± SD. Statistical significance was tested by unpaired Student's *t*-test. $^*p < 0.05$, $^{**}p < 0.01$, and $^{***}p < 0.001$.

Figure 7. PLCE1 knockdown inhibits ESCC metastasis in nude mice

ECA-109 cells were transduced with lentivirus bearing PLCE1 shRNA (LV-shPLCE1) or NC shRNA (LV-shPLCE1 NC). Each mouse was intravenously injected with the LV transduced cells (1 x 10^6 cells/mouse). Eight weeks later, mice were sacrificed, and the lungs and livers from each group were collected and photographed.

(A) Typical images of lung specimens.

(B) Hematoxylin and eosin staining of metastatic nodules in lungs.

(C) The number of nodules in lungs.

(D) PLCE1 knockdown represses signal transduction in the axis of PKC/GSK-3β/β-Catenin. Protein levels were analyzed by western blot, and Actin was used as a loading control. $n = 3$ biologically independent replicates.

(E) Quantitative analysis of the western blot data shown in (D).

Data are presented as mean ± SD. Statistical significance was tested by unpaired Student's *t*-test. $^{**}p < 0.01$, and $^{***}p < 0.001$.

FIGURE 1

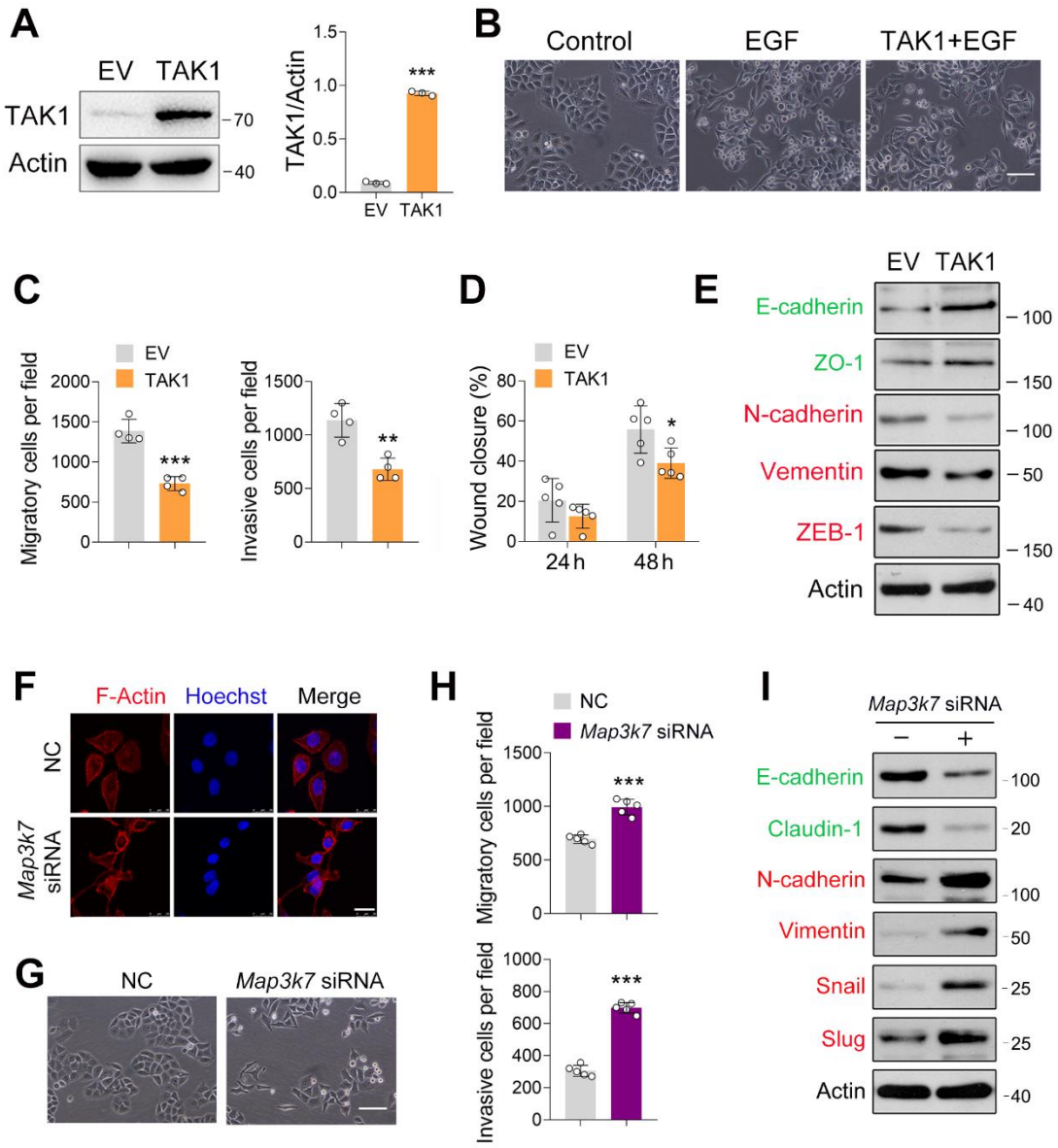
A
EV TAK1
TAK1
Actin
70
40
TAK1/Actin
1.5
1.0
0.5
0.0
***
EV TAK1
B
Control
EGF
TAK1+EGF
C
EV
TAK1
Migratory cells per field
2000
1500
1000
500
0
***
Invasive cells per field
1500
1000
500
0
**
D
EV
TAK1
Wound closure (%)
80
60
40
20
0
*
24 h
48 h
E
EV TAK1
E-cadherin
ZO-1
N-cadherin
Vementin
ZEB-1
Actin
100
150
100
50
150
40
F
F-Actin
Hoechst
Merge
NC
Map3k7 siRNA
G
NC
Map3k7 siRNA
H
NC
Map3k7 siRNA
Migratory cells per field
1500
1000
500
0
***
Invasive cells per field
1000
800
600
400
200
0
***
I
Map3k7 siRNA
−
+
E-cadherin
Claudin-1
N-cadherin
Vimentin
Snail
Slug
Actin
100
20
100
50
25
25
40

933 FIGURE 2

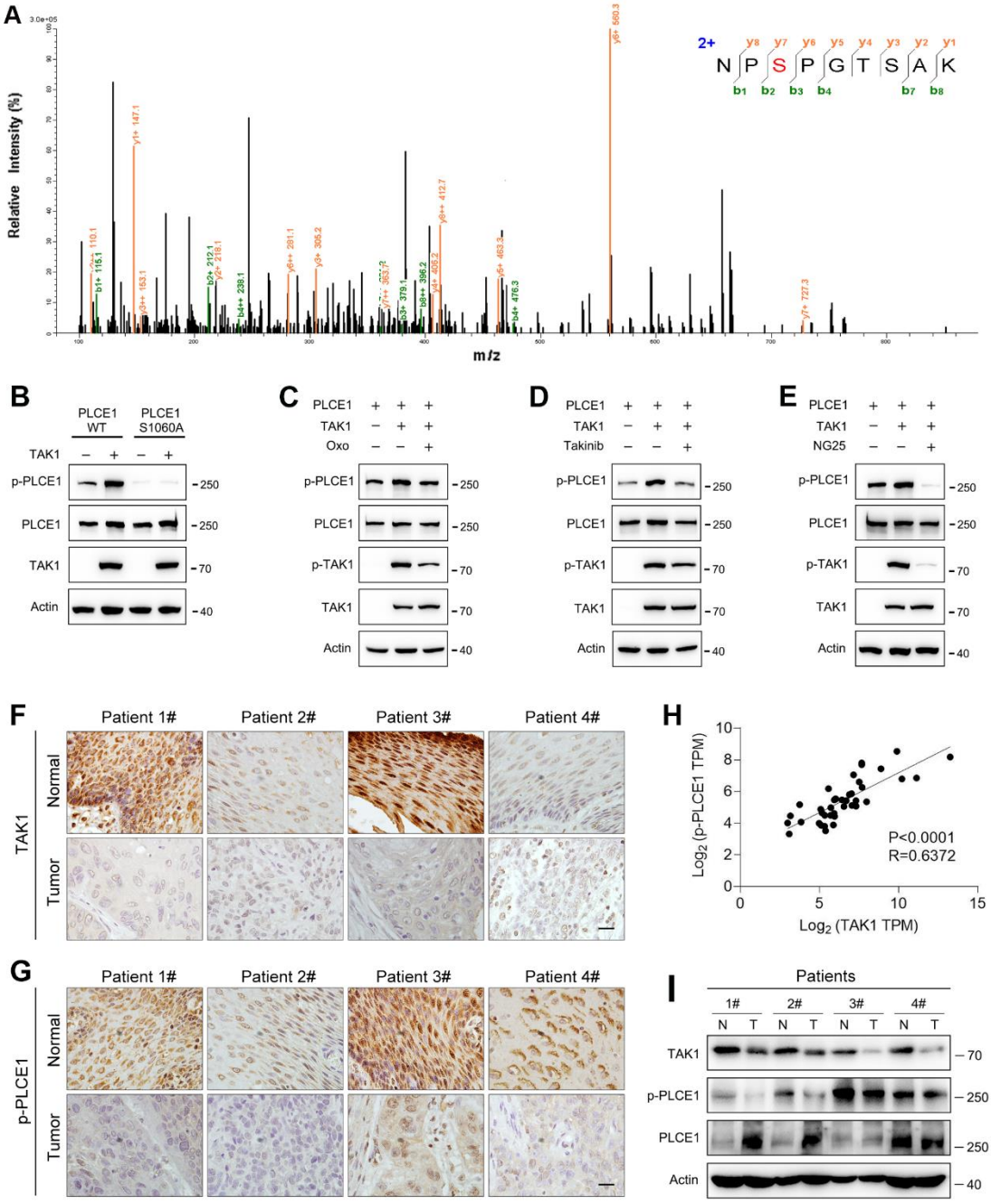

934

935

936

937

938

939

940

941

FIGURE 3

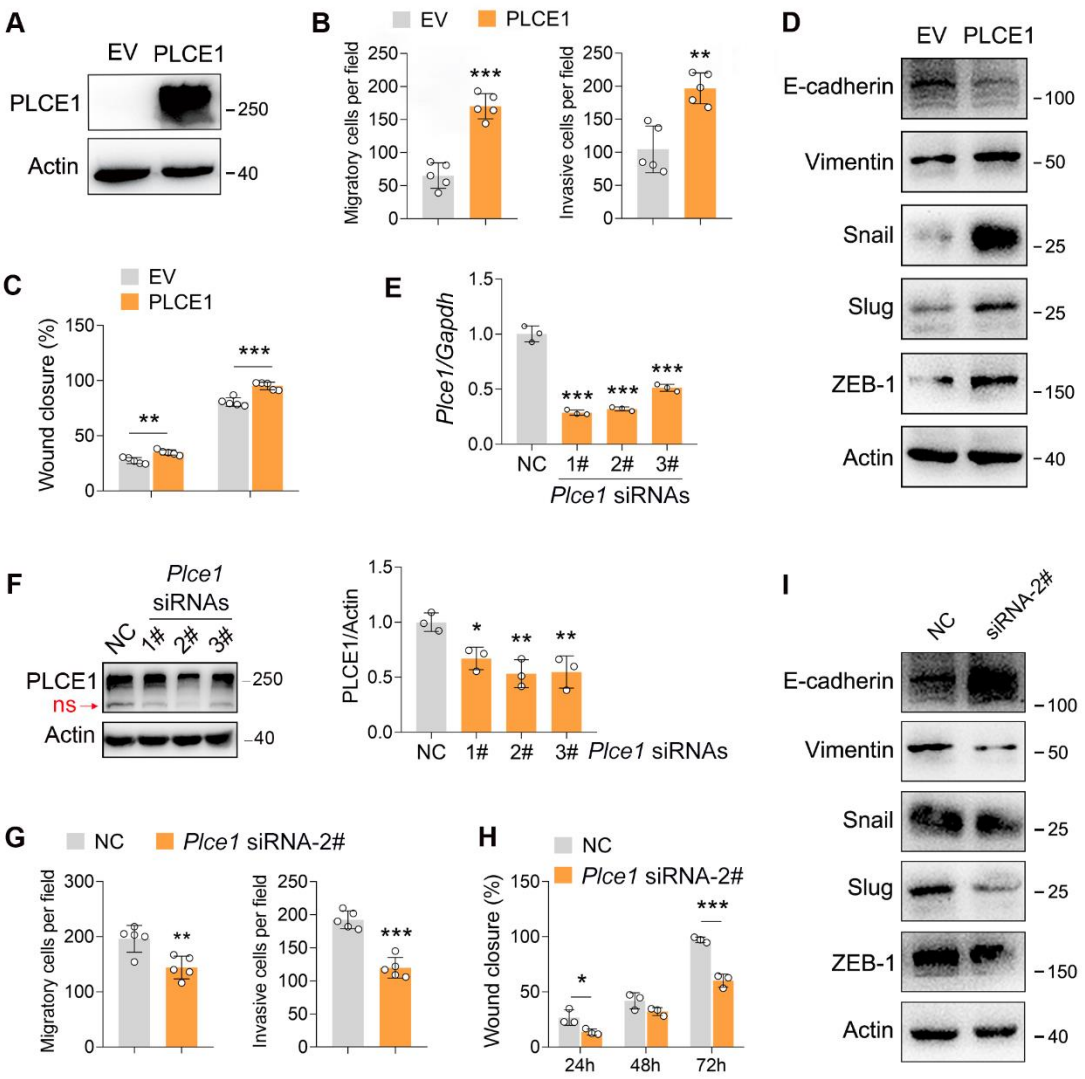
A
EV PLCE1
PLCE1
Actin
250
40
B
EV
PLCE1
Migratory cells per field
Invasive cells per field
C
Wound closure (%)
D
E-cadherin
Vimentin
Snail
Slug
ZEB-1
Actin
100
50
25
150
40
E
Plce1/Gapdh
NC 1# 2# 3#
Plce1 siRNAs
F
Plce1 siRNAs
NC 1# 2# 3#
PLCE1
ns
Actin
PLCE1/Actin
G
NC
Plce1 siRNA-2#
H
Wound closure (%)
24h 48h 72h
I
NC
siRNA-2#

FIGURE 4

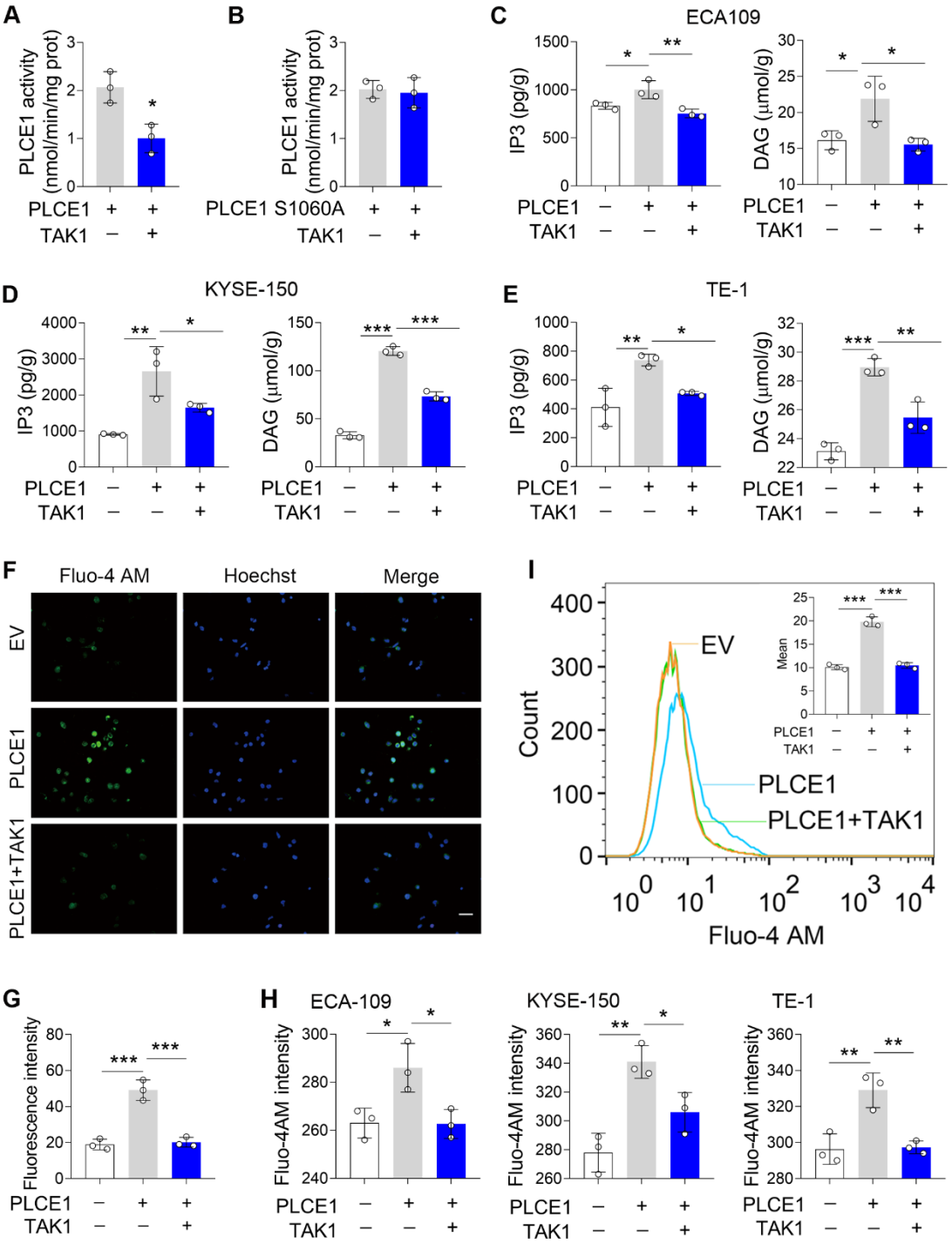
A
PLCE1 activity (nmol/min/mg prot)
PLCE1
TAK1
B
PLCE1 activity (nmol/min/mg prot)
PLCE1 S1060A
TAK1
C
ECA109
IP3 (pg/g)
DAG (μmol/g)
PLCE1
TAK1
D
KYSE-150
IP3 (pg/g)
DAG (μmol/g)
PLCE1
TAK1
E
TE-1
IP3 (pg/g)
DAG (μmol/g)
PLCE1
TAK1
F
Fluo-4 AM
Hoechst
Merge
EV
PLCE1
PLCE1+TAK1
I
Count
Fluo-4 AM
EV
PLCE1
PLCE1+TAK1
Mean
PLCE1
TAK1
G
Fluorescence intensity
PLCE1
TAK1
H
ECA-109
KYSE-150
TE-1
Fluo-4AM intensity
PLCE1
TAK1

962 FIGURE 5

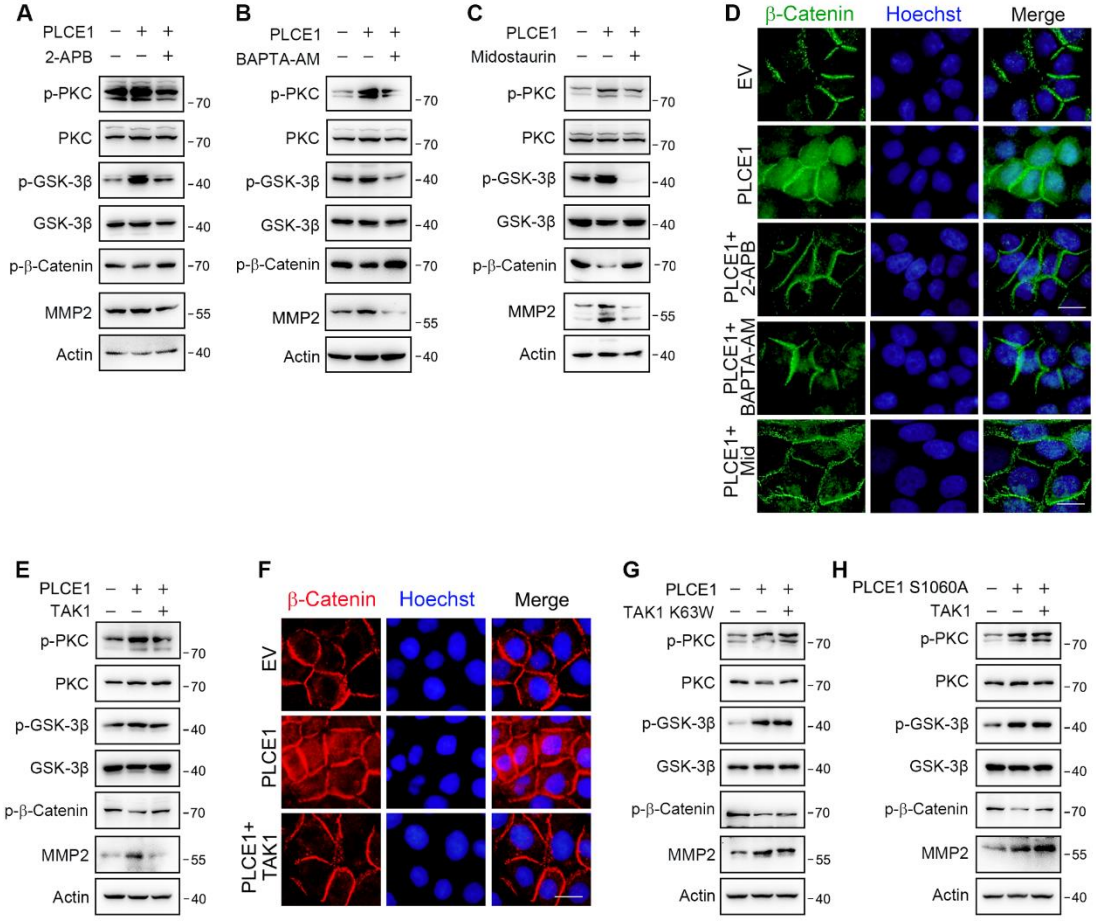

963

964

965

966

967

968

969

970

971

972

973

974

975

976

977 FIGURE 6

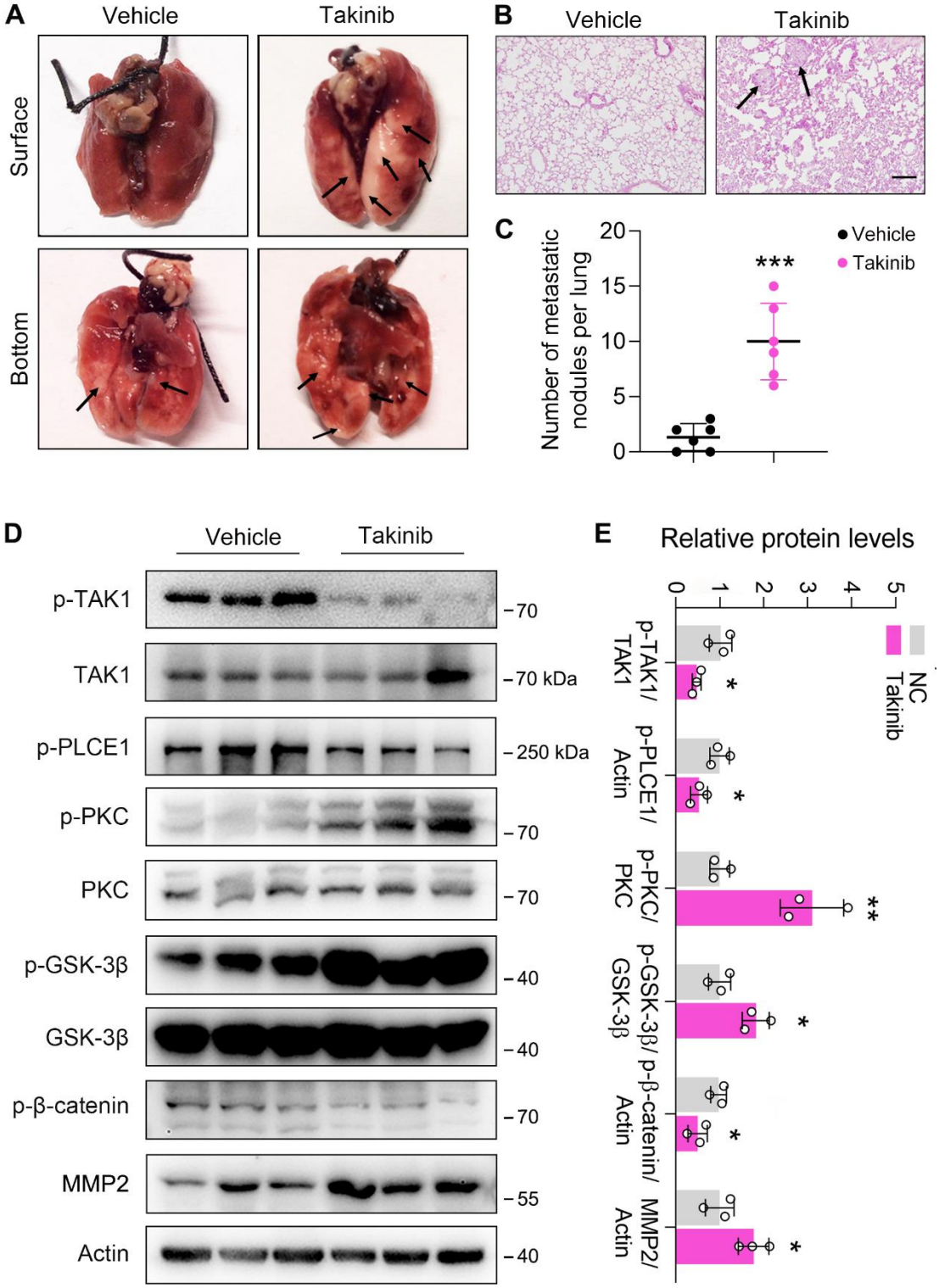

978

979

980

981

982 FIGURE 7

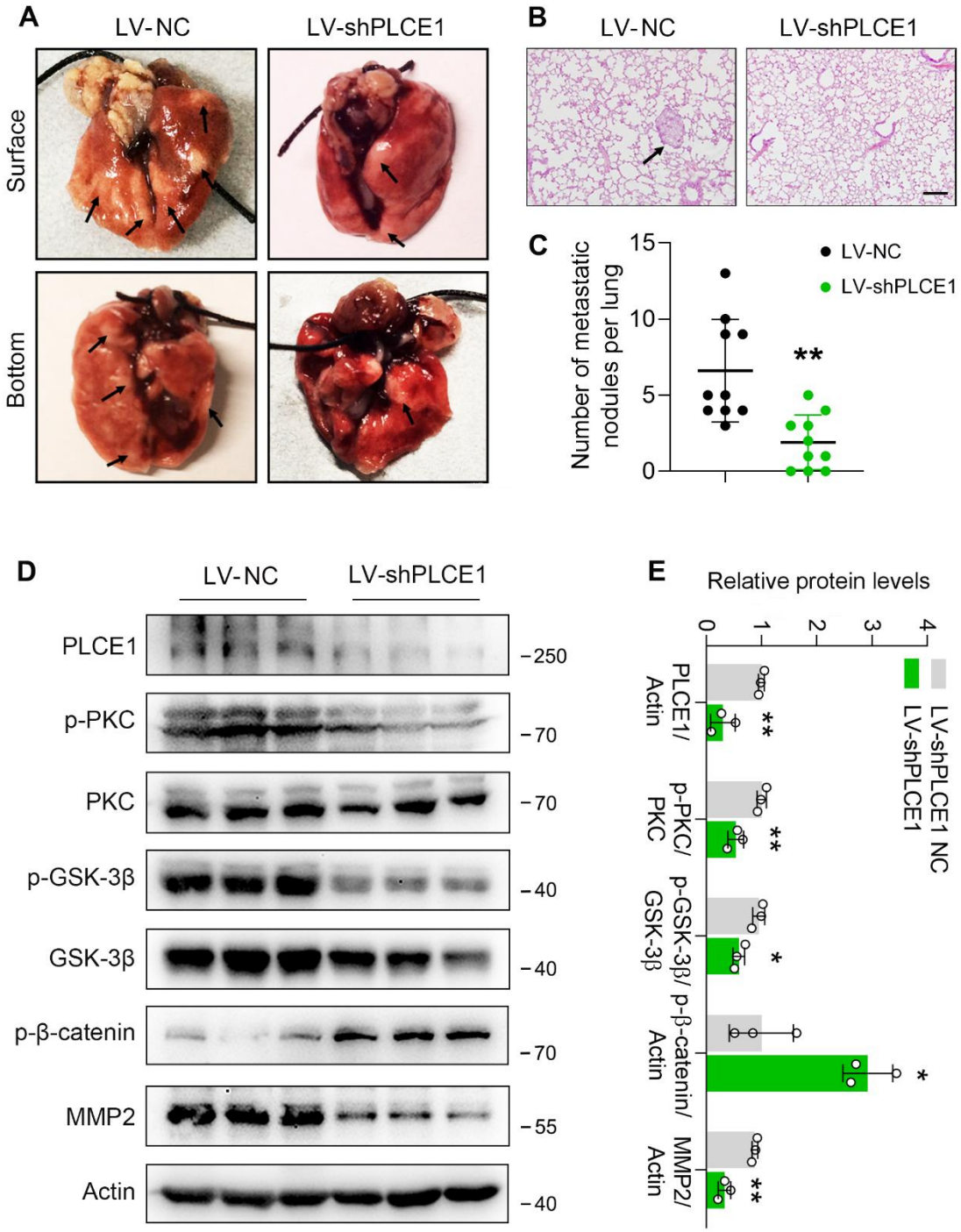

983

984